Fractal Analysis of Flame-Synthesized Nanostructured Silica and Titania Powders Using Small-Angle X-ray Scattering

Jingyu Hyeon-Lee,[†] Gregory Beaucage,*[,†] Sotiris E. Pratsinis,[‡] and Srinivas Vemury[§]

Department of Materials Science and Engineering, ML 0012, and Department of Chemical Engineering, ML 0171, University of Cincinnati, Cincinnati, Ohio 45221, and Lucent Technologies, G010, 2000 Northeast Expressway, Norcross, Georgia 30071

Received March 17, 1998. In Final Form: July 21, 1998

The morphology of flame-generated silica and titania aggregates is characterized by small-angle X-ray scattering (SAXS). Nearly all these powders display mass-fractal morphologies, which are composed of ramified aggregates of nanoscale primary particles. Primary particle size, aggregate size, fractal dimension, and specific surface area are obtained from this analysis. The mass-fractal dimension varies from 2.5 to 1.6 for flame generated silica and titania aggregates in single and double diffusion flame reactors. However, titania powders made in a single diffusion flame reactor appear as nonaggregates and nonfractals. Silica powders synthesized with an imposed electric field in a laminar, premixed flame reactor are mass fractals with narrowly confined fractal dimensions from 1.5 to 1.9 regardless of aggregate size.

Introduction

Aggregates of small primary particles can be produced by various aerosol processes, including flame processes for the production of materials such as titania, fumed silica, and carbon black. During these processes, structural features such as particle and aggregate size, structure, and surface area vary, affecting the properties of the final product.[1] Although aggregation behavior on molecular or colloidal scales is important, relatively little attention has been paid to it, partly because of the highly disordered nature of these materials and difficulties in characterization. However, with fractal concepts, the description of morphological features of aggregates has been facilitated.

The primary tools for description of the morphology of aggregates using fractals are electron microscopy[2−5] and X-ray[6−9] or light scattering.[10,11] Megaridis and Dobbins obtained a fractal dimension of about 1.7 for flame-generated carbonaceous soot and fumed silica based on transmission electron microscopy (TEM), suggesting that cluster−cluster aggregation is an important growth mechanism. More recently, Koylu et al.[3] analyzed flame synthesized carbonaceous soot and found that aggregates are mass-fractal with fractal dimension (d_f) of about 1.7. Although microscopy is quite useful in measurements of primary particle size, it is generally difficult to obtain primary particle size distribution from microscopy and the measurement thus relies on a tedious process of micrograph measurements. Microscopic characterization of the morphology of secondary, mass-fractal structures is even a more difficult and subjective process. Moreover, the occlusion of 3-dimensional structure by overlap of a number of aggregates or even superimposed structure from the same aggregate, in a typical micrograph, makes the process quite difficult.

Small-angle X-ray scattering (SAXS) offers an alternate to this process since it is by nature a 3-dimensional averaging technique with a direct measure of the radius of gyration, R_g. Characterization of 3-dimensional mass-fractal morphologies is simple in a typical scattering experiment. Combustion aerosol aggregates have been characterized using SAXS in terms of a statistical analysis.[6−9] Schaefer et al.[6] obtained fractal dimensions between 1.7 and 1.9 for fumed silica aggregates from SAXS and found that the surface of fumed silica is self-affine with surface fractal dimensions between 2.5 and 3. For these flame-generated silica powders, the features of kinetic growth processes were also suggested. In addition to SAXS, ultra small-angle X-ray scattering (USAXS) scattering patterns can be extended to close to the millimeter size scale by careful combination of SAXS data with light scattering data. In the past, such combined scattering curves and global scattering functions[12−14] have been used to describe the three levels of structure for fine powders, primary, secondary (aggregate) and tertiary (agglomerate).[12−14]

Fumed silica and titania powders made in a diffusion flame reactor and a laminar, premixed flame reactor are analyzed in this study. When particles are synthesized in these reactors, the characteristics of the flame such as mixing configuration or oxidant type can greatly affect

[†] Department of Materials Science and Engineering, University of Cincinnati.
[‡] Department of Chemical Engineering, University of Cincinnati.
[§] Lucent Technologies.

(1) Pratsinis, S. E. *Prog. Energy Combust.* **1998**, *24* (3), 197.
(2) Megaridis, C. M.; Dobbins, R. A. *Combust. Sci. Technol.* **1995**, *71*, 95.
(3) Koylu, U. O.; Xing, Y.; Rosner, D. E. *Langmuir* **1995**, *11*, 4848.
(4) Neimark, A. V.; Koylu, L. O.; Rosner, D. E. *J. Colloid Interface Sci.* **1996**, *180*, 590.
(5) Samson, R. J.; Mulholland, G. W.; Gentry, J. W. *Langmuir* **1987**, *3*, 272.
(6) Schaefer, D. W.; Hurd, A. J. *Aerosol Sci. Technol.* **1990**, *12*, 876.
(7) Schaefer, D. W.; Keefer, K. D. In *Fractals in Physics*; Pietronero, L., Tosatti, E., Eds.; Elsevier Science: Amsterdam, 1986; p 39.
(8) Schaefer, D. W. *Mater. Res. Symp. Proc.* **1987**, *79*, 47.
(9) Schaefer, D. W.; Martin, J. E.; Wiltzius, P.; Cannell, D. S. *Phys. Rev. Lett.* **1984**, *52*, 2371.
(10) Oh, C.; Sorensen, C. M. *J. Aerosol Sci.* **1997**, *28* (6), 937.
(11) Hurd, A. J.; Flower, W. L. *J. Colloid Interface Sci.* **1988**, *122* (1), 178.
(12) Beaucage, G.; Schaefer, D. W. *J. Non-Cryst. Solids* **1994**, *172−174*, 797.
(13) Beaucage, G. *J. Appl. Cryst.* **1995**, *28*, 717.
(14) Beaucage, G. *J. Appl. Cryst.* **1996**, *29*, 134.

S0743-7463(98)00308-4 CCC: $15.00
Published on Web 08/26/1998

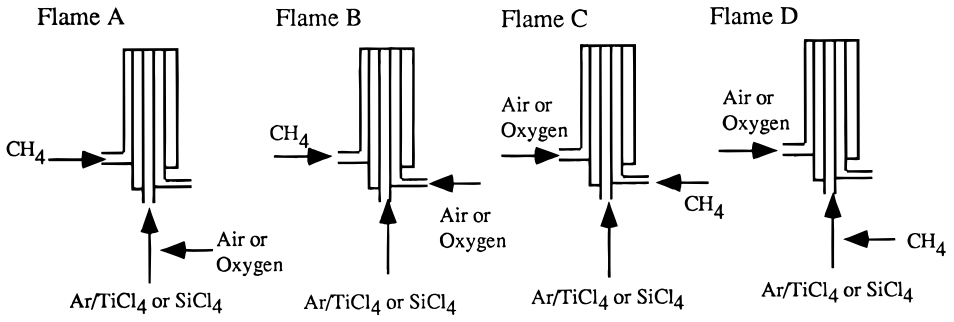

Figure 1. Reactant gas mixing configurations for diffusion reactors.[15]

particle characteristics through the growth process. Moreover, when an electric field is imposed across the flame, it can cause a profound effect on primary particle size, degree of aggregation and other morphological features such as fractal dimensions. Morphological features, fractal dimension (d_f), radius of gyration of primary particles (R_{g1}), radius of gyration of aggregate (R_{g2}), and specific surface area (S) of flame-generated powders are thus investigated using small-angle X-ray scattering (SAXS) with the unified fitting approach.[12−14] The effects of flame configuration and oxidant type in a diffusion reactor are considered as well as the effects of externally controlled electric fields in a laminar, premixed flame reactor. Data obtained by SAXS, moreover, are compared with previous data measured by nitrogen adsorption (BET) and TEM.[15−17]

Experimental Methods

Silica and titania powders were synthesized in a diffusion flame reactor,[15,16] and a laminar, premixed flame reactor.[17] Powders are made at different oxidant and flame configurations (Figure 1) in a diffusion flame reactor. Silica powders were also produced with an electric field across the laminar flow reactor using either needle electrodes that introduce ions in the flame or plate electrodes that merely attract flame-generated ions.[18] The electric field was either positive or negative. In the case of negative or positive electric field, one electrode is connected to the dc power supply (negative or positive) and the other one to the ground. The precursors for silica and titania are $SiCl_4$ and $TiCl_4$, respectively, and were delivered as vapors at a controlled rate. The silica and titania powders were collected on glass fiber filters using a vacuum pump. Additional experimental details can be found in the literature.[15−18]

Small-angle X-ray scattering (SAXS) data were collected with a Bonse-Hart camera at the Sandia/UNM scattering center in Albuquerque, NM. The data were desmeared prior to fitting. These ultra-small-angle X-ray scattering (USAXS) experiments extend the SAXS region to approximately 1 μm in size. The q range covered is from about 0.00015 to 0.6 Å^{-1}. The momentum transfer vector, q, has units (length)$^{-1}$ so large-q scattering probes small length-scales.

Theoretical: Data Analysis. In this section, the unified fitting approach to determine parameters such as R_g or d_f is summarized.[12−14] Aggregates can be described as mass-fractals. Under a mass-fractal model, the fractal dimension d_f describes, statistically, the geometry of many random objects, and is widely used to describe scaling laws in small-angle scattering. The d_f is defined by[19]

$$M(R) \propto R^{d_f} \quad (1)$$

where M is the mass of material contained in a sphere of radius R centered at an arbitrary point on the object. The fractal dimension falls in the range $1 \le d_f < 3$ (objects with $d_f = 3$ do not display mass-fractal scattering contrast). For example, the fractal dimension of a rod is taken as 1 because the mass is proportional to the length. Similarly, the fractal dimensions of a thin disk and a sphere are 2 and 3, respectively. Fractal morphologies over a limited range of size R satisfying eq 1 are often found in aerosol aggregates between the primary particle size and the aggregate size.

The fractal dimension can be obtained experimentally from small-angle X-ray scattering (SAXS) measurements. The d_f is measured from the negative slope of log(intensity) vs log(magnitude of the scattering vector), q, in a power-law regime, where $q = 4\pi/\lambda \sin(\theta/2)$, θ is the scattering angle, and λ is the wavelength. We use the unified equation[12−14] to describe the limits to mass-fractal scaling at the aggregate radius of gyration R_{g2} and the primary particle radius of gyration R_{g1}. The radius of gyration is defined as the mean square distance from the center of gravity where the role of mass is played by the electron density,[20] which is expressed as

$$R_g = [\sum_{i=0}^{\infty} C_i (R_i)^2 / \sum_{i=0}^{\infty} C_i]^{1/2} \quad (2)$$

where R_i is the distance from the center for the volume element i of contrast C_i. Specific relations between the dimensions of a particle and R_g are available, depending on the model used to describe the particle, i.e., for a sphere, diameter $(D) = 2(5/3)^{1/2} R_g$.[21] The unified equation under mass-fractal constraints[14] is further constrained by assuming spherical primary particles.

The unified approach breaks a complex scattering pattern into structural levels, each of which contains a Guinier regime reflecting the R_g, and particle contrast followed by a power-law regime which describes the type of structures to which the Guinier regime pertains. For mass-fractal aggregates there are two structural levels: the first pertaining to the primary particles (ca. 100 Å) and the second to the mass-fractal aggregates (ca. 500 Å). Each structural level is described, in the unified approach, by four generic parameters, G, R_g, B, and P, which can be calculated from limiting cases of known scattering laws or limits of integral equations in the case of mass-fractals. For a mass fractal, G is a constant defined by the specifics of the primary particle (G_1) or aggregate compositions (G_2), and is given by[14]

$$G_2 = N_{agg} \Delta n_{e\ agg}{}^2 = (N_{pp}/z)(z\Delta n_{e\ pp})^2 = z\, N_{pp} (\Delta n_{e\ pp})^2 = z\, G_1 \quad (3)$$

where N_{agg} is the number of aggregates in the scattering volume, N_{pp} is the number of primary particles in the scattering volume, $\Delta n_{e\ agg}$ is a contrast factor for aggregates, $\Delta n_{e\ pp}$ is a contrast factor for primary particles, and z is the degree of aggregation

(15) Pratsinis, S. E.; Zhu, W.; Vemury, S. *Powder Technol.* **1996**, *86*, 87.
(16) Zhu, W.; Pratsinis, S. E. In *Nanotechnology*; Chow, G.-M., Gonsalves, K. E., Eds.; American Chemical Society: Washington, DC, 1996; p 64.
(17) Vemury, S.; Pratsinis, S. E. *J. Aerosol, Sci.* **1996**, *27* (6), 951.
(18) Vemury, S.; Pratsinis, S. E.; Kibbey, L. *J. Mater. Res.* **1997**, *12* (4), 1031.
(19) Mandelbrot, B. B. *The Fractal Geometry of Nature*; W. H. Freeman & Co: New York, 1983; Chapter 34.
(20) Glatter, O.; Kratky, O. *Small-Angle X-ray Scattering*; Academic Press: New York, 1982; p 25.
(21) Hiemenz, P. C. *Principles of Colloid and Surface Chemistry*; Marcel Dekker: Inc.; New York, 1977; p 192.

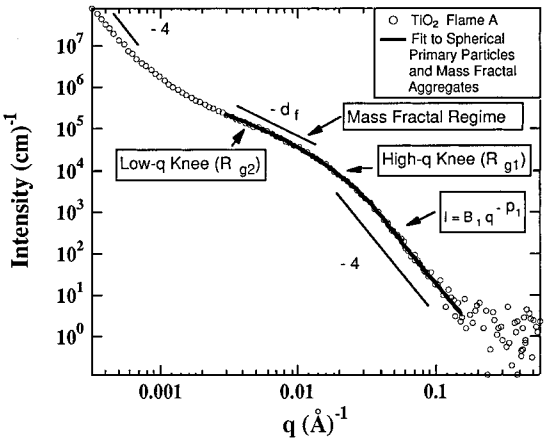

Figure 2. Typical data and fit for titania powders made in flame A with air as oxidant in diffusion flames.

(number of primary particles in an aggregate). The radius of gyration, R_{g2}, for a mass fractal with mass-fractal dimension d_f, and degree of aggregation, z, is given by[14]

$$R_{g2} = \{b^2 z^{2/d_f}/[(1 + 2/d_f)(2 + 2/d_f)]\}^{1/2} \quad (4)$$

where b is the primary particle size, and $b = 2R$.[14] *"R"* is defined as the radius of primary particle. B is a prefactor specific to the type of power-law scattering.[14] The power-law prefactor B for mass-fractal aggregates is given by[14]

$$B_2 = (G d_f/R_{g2}^{d_f})\Gamma(d_f/2) \quad (5)$$

where Γ is the gamma function. P is the power-law slope, and $P = -d_f$. For spherical primary particles of radius R, $G_1 = N_{pp}\Delta n_{e\ pp}^2$, $R_{g1} = (3/5)^{1/2}R$, and $B_1 = N_{pp}2\pi\Delta\rho_e^2 S_{pp} = N_{pp}2\pi(\Delta n_{e\ pp}^2/V_{pp}^2)S_{pp}$, where $\rho_e = n_{e\ pp}/V_{pp}$, $n_{e\ pp}$ is the number of electrons in a primary particle, V_{pp} is the volume of primary particle, and S_{pp}, $4\pi R^2$, is the surface area for the spherical primary particle. Thus a mass fractal with spherical primary particles is described by four parameters; z, R_{g1}, d_f, and G_1, under this model. The surface area can also be determined for the mass-fractal scaling regime of the small-angle scattering pattern. To calculate the surface area, the volume of the substructural unit[14] needs to be determined from the Porod invariant, Q, and Guinier prefactor, G_1:

$$Q = \int_0^\infty I(q)q^2\, dq = 2\pi^2 G_1/V_{pp} \quad (6)$$

$$B_1 = 2\pi(G_1/V_{pp})(S_{pp}/V_{pp}) \quad (7)$$

where G_1 and Q can be obtained from the scattering pattern. The surface-to-volume ratio, (S_{pp}/V_{pp}), can be described as

$$S_{pp}/V_{pp} = B_1 V_{pp}/2\pi G_1 = \pi B_1/Q \quad (8)$$

From these equations, the specific surface area (S_{pp}/mass) for nanoscale silica and titania powders are calculated using $(S_{pp}/\text{mass}) = (S_{pp}/V_{pp})(1/\rho)$, where ρ_{silica} is 2.2 g/cm^3 and $\rho_{titania}$ is 4.07 g/cm^3, respectively.

Results and Discussion

TiO_2 Powders Made in Diffusion Flames. Figure 2 shows a typical SAXS profile for TiO_2 powders synthesized with the flow rates of CH_4, air, and Ar as 312, 3800, and 250 cm^3/min, respectively, while $TiCl_4$ was kept at room temperature[15] in a double diffusion flame. The scattering patterns show 3 power-law regimes: At high-q, a power-law of -4 is observed for the surface of the primary particle. At intermediate-q, a weak slope corresponds to a mass fractal regime. At low-q, a power-law of -4 is observed for mass-fractal agglomerates of aggregates. The agglomerate regime was ignored in this work. Mass fractal scattering of arbitrary mass fractal dimension d_f can be described by four parameters (G_1, d_f, R_{g1}, and z as described above). The data display eight distinguishable features, G_1, B_1, P_1, R_{g1}, G_2, B_2, R_{g2}, and d_f. The determination of degree of aggregation is sometimes difficult by the interference from the Porod tail of agglomerates, i.e., G_2 and R_{g2} are obscured. In all cases at least six clearly distinguishable parameters, the high-q power law prefactor B_1, P_1, R_{g1}, G_1, d_f, and low-q power law prefactor B_2, are observed, from which the four parameters of the model, G_1, d_f, R_{g1}, and z, are obtained.

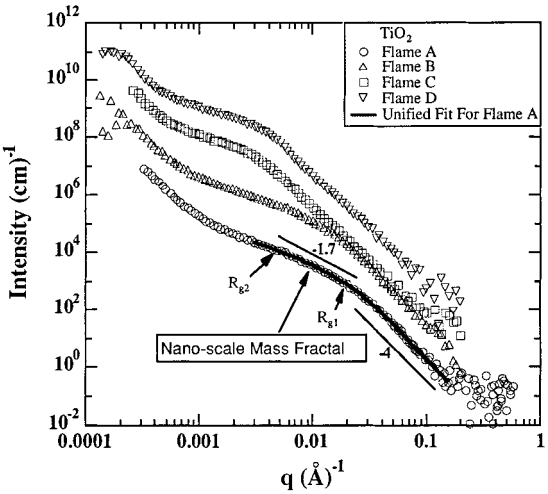

Figure 3. X-ray scattering data from TiO_2 powders generated in different flame configurations. The scattering data for flame D and flame C have been multiplied by factors of 100 and 10, respectively. The scattering data for flame A have been divided by a factor of 10.

Table 1. Properties of TiO_2 Powders Synthesized in Different Flame Configurations by SAXS

flame	R_{g1} (Å)	D_{sphere} (Å)	R_{g2} (Å)	S (m^2/g)	d_f	z
A	54	139	615	217	1.72	67
B	88	227	695	130	1.60	29
C	829	2140	–	19	–	–
D	800	2066	–	22	–	–

Figure 3 shows a plot of intensity vs magnitude of the scattering vector, q, for titania aggregates generated from the four flame configurations, shown in Figure 1. As noted above, two structural levels are displayed in the scattering profile for flame A: The lower and upper limits of the mass fractal power-law regime are characterized by the radius of gyration of primary particle (R_{g1}), and aggregate (R_{g2}), which appear as a high-q knee ($q \approx 0.02$) and a low-q knee ($q \approx 0.004$), respectively. As the flame configuration changes from A to B, C, and D, the high q knees (R_{g1}) shift to lower-q, corresponding to larger primary particles. Using a sphere model for the base unit of the mass-fractal chain $R_{sphere} = (5/3)^{1/2}R_{g1}$, the mean diameter, $D_{sphere} = 2R_{sphere}$, of primary particles is obtained. The R_{g2} for a mass fractal with fractal dimension d_f is given by eq 4. Surface areas are calculated using the volume of the smallest unit which is obtained from eq 8.

Table 1 shows the results obtained from the SAXS data analysis of Figure 3. Titania powders synthesized under flame configuration A have the smallest primary particle size among all flame configurations. The average diameter of titania primary particle generated in flame A is 139 Å as determined by SAXS. In the flame A configuration, the $TiCl_4$ vapor stream is vigorously diluted[15] with air prior to its oxidation in the flame. The flame temperatures

in flame A and B were 966 and 998 °C with flame heights of 38 and 55 mm, respectively.[15] Dilution causes lower flame temperature and particle sintering rates in flame A, leading to less growth of primary particles at early stage, resulting in the smallest primary particles. Compared to flame A, particles made in flame B experience limited dilution and higher temperature, resulting in larger primary particles, 227 Å. These results are in good agreement with TEM and BET analyses that gave average primary particle sizes of 11 and 25 nm for titania made[15] in flames A and B, respectively.

Titania powders synthesized in these two flame configurations show mass-fractal morphologies. The radius of gyration of titania aggregates in flame A, R_{g2}, is around 615 Å, consisting of primary particles R_{g1} 54 Å and fractal dimension of 1.72 with a mean degree of aggregation (z) of 67 per aggregate. The radius of gyration of titania in flame B, R_{g2}, is around 695 Å, being composed of primary particles R_{g1} 88 Å and fractal dimension of 1.60 with an average degree of aggregation (z) of 29 per aggregate. The degree of aggregation is higher in flame A than flame B, due to the relatively lower temperature and shorter particle residence time at high temperatures in flame A. The growth of these aggregates generated in flames A and B follows diffusion-limited cluster−cluster aggregation process, with fractal dimensions of 1.8 for clusters as have been shown by simulations.[22] The fractal dimensions measured by SAXS, 1.72 and 1.6, are reasonably close to that value.

However, there is a drastic difference in primary particle and aggregate size between flame configurations A/B and C/D. The average diameters of primary particles generated in flames C and D are near 2100 Å. The temperatures in flame C and D were about 1020 °C at almost the same flame height (about 73 mm).[15] Mass fractal aggregates generated in flames A and B have much higher specific surface areas than those generated in flames C and D, consistent with much smaller primary particles in flames A and B. Furthermore, mass fractal morphologies are not observed for powders made in flames C and D by SAXS (Figure 3). Particles generated in flames C and D grow at high temperatures and experience high sintering rates, so colliding particles fuse quickly. Microscopy reveals that these particles are quite spherical and clearly not mass-fractal, especially when pure oxygen is used as oxidant (e.g. Figure 5 in Zhu and Pratsinis[16]). These SAXS observations are consistent with observations by TEM.[15,16]

SiO_2 Powders Made in Diffusion Flames. Figure 4 shows the scattering profile of SiO_2 powders generated in diffusion flames A and D using oxygen or air as oxidant with flow rates of CH_4, air, and Ar of 400, 3800, and 250 cm^3/min, respectively. When oxygen was used as oxidant, the flow rate of oxygen was the same as that of air. Flame A_{Air} designates flame configuration A with air as oxidant, and flame A_{Oxy} is flame configuration A with oxygen as oxidant in Figure 4. D_{Air} and D_{Oxy} also mean flame configuration D with air and oxygen as oxidants, respectively. The scattering patterns display two structural levels at all conditions. At low-q, a large-scale structure is present that displays mass-fractal scaling. At high-q, spherical substructures limit the mass fractal power-law regime. For oxygen as oxidant, the high-q knee which corresponds to the primary particle size (R_{g1}), moves to lower-q when the flame configuration changes from a low-temperature double diffusion flame A to a high-temperature single diffusion flame D. Moreover, the high-q knee for flame D_{Oxy} is located to the left compared to the high-q knee for flame D_{Air}, suggesting that oxygen generates larger primary particles than air in flame D. The measured primary particle and aggregate sizes, the degree of aggregation, and specific surface area from SAXS are summarized in Table 2.

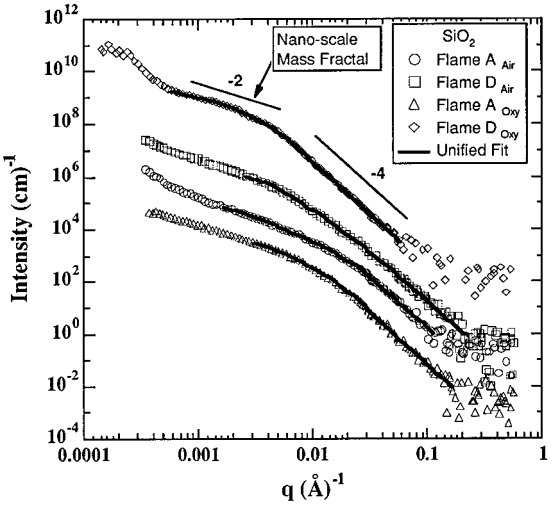

Figure 4. X-ray scattering data from SiO_2 powders generated in different flame configuration/oxidants. The scattering data for flame D_{Oxy} have been multiplied by a factor of 100. The scattering data for flame A_{Oxy} and A_{Air} have been divided by factors of 100 and 10, respectively.

Table 2. Fractal Properties of SiO_2 Powders Synthesized in Different Flame Configurations/Oxidants by SAXS

flame	oxidant	R_{g1} (Å)	D_{sphere} (Å)	R_{g2} (Å)	S (m^2/g)	d_f	z
A_{Oxy}	oxygen	91	232	415	26	2.31	27
A_{Air}	air	72	186	982	348	1.90	135
D_{Oxy}	oxygen	370	955	2630	70	1.65	27
D_{Air}	air	80	207	517	303	2.48	72

Flame A_{Oxy} generates smaller primary particles and aggregates compared to flame D_{Oxy} when oxygen is used as oxidant. The average diameter (D) of primary particles in flame A and D are 232 and 955 Å, respectively. A similar trend was observed for titania powders (Figure 3): a dilution effect and lower temperature seem to contribute to the production of smaller silica particles in flame A.

When oxygen rather than air is used as oxidant in the same flame configuration, silica powders have larger size in both primary particles and aggregates. Compared to the air flame, pure oxygen accelerates fuel consumption, leading to an increase in flame temperature of about 500 °C. Particles generated in oxygen flames, which leads to fast sintering, have 3−4 times larger primary particle sizes (D_{sphere} in Table 2) than those in air flames, especially under flame configuration D. The oxidant effect is more dramatic in flame D than in flame A because dilution contributes significantly to reducing the reaction temperatures and sintered particle sizes in flame A. Both flames A and D generate smaller primary particles when air is used as oxidant, leading to powders of high specific surface area.

The silica powders are mass fractals. The larger aggregates generated in flame A_{Air} and flame D_{Oxy} seem to form more open chainlike fractals with larger collision radii, with fractal dimensions around 1.8 (1.65−1.90), consistent with 1.8 for diffusion limited cluster−cluster aggregation. Relatively smaller aggregates of these silica powders generated in flame A_{Oxy} and D_{Air} form more

(22) Meakin, P. In *On Growth and Form*; Stanley H. E., Ostrowsky N., Eds.; Martinus-Nijhoff: Boston, 1986; p 111.

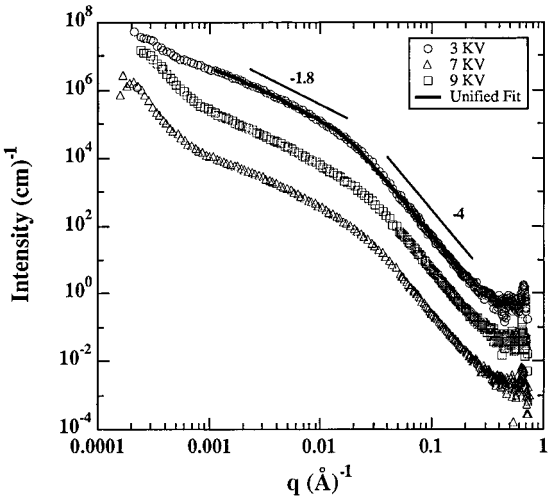

Figure 5. X-ray scattering data from a series of SiO_2 powders generated with a negative electric field in a laminar, premixed flame reactor.

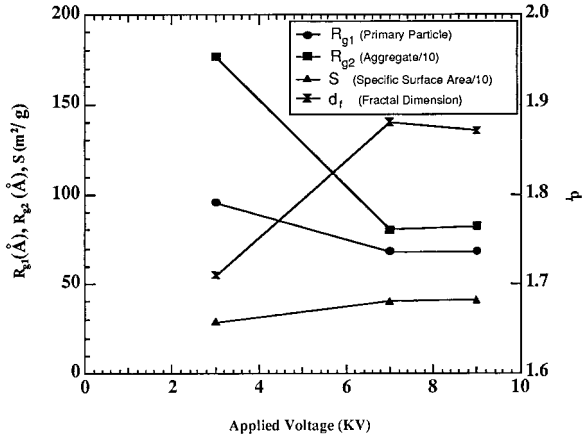

Figure 6. Radius of gyration of primary particle R_{g1}, radius of gyration of aggregates R_{g2}, specific surface area S, and fractal dimension d_f as a function of applied voltage across the flame for negative electric field with plates. The R_{g2} and S data have been divided by 10.

compact branched fractals, with fractal dimensions of 2.4, which follows a diffusion-limited monomer−cluster aggregation process suggested by Witten and Sanders.[23] In diffusion limited monomer−cluster aggregation process, randomly traveling monomers by Brownian motion stick irreversibly at first when they contact growing clusters. Because of their Brownian trajectories, these monomers cannot penetrate deeply into a cluster without interpenetrating a cluster arm. The arms effectively screen the interior from the flux of incoming monomers: therefore, growth preferentially occurs at exterior sites resulting in mass fractal objects.[24]

SiO_2 Powders Made in an Electrically Assisted Laminar, Premixed Flame Reactor. The presence of external electric fields can facilitate flame synthesis of particles with closely controlled characteristics.[17,18] Figure 5 shows the scattering profile of intensity vs magnitude of the scattering vector, q, for SiO_2 powders made in a premixed flame reactor at these potential differences of a negatively charged plate/plate electrode across the burner with flow rates of air, O_2, and CH_4 fixed at 4300, 240, and 445 cm^3/min, respectively, while 100 cm^3/min of argon is bubbled through the $SiCl_4$ containing flask.[17] In a premixed flame, the fuel and oxidant are mixed prior to reaching the burner so nearly all particles experience the same temperature, gas-phase composition, and residence time.[25] In the scattering pattern, two structural levels of chainlike fractals are observed, which are obtained using the unified equation. Figure 5 shows that, when the field intensity across the flame is increased from 3 to 9 kV, the high-q knee (R_{g1}) shifts from lower-q to higher-q, implying that primary particle size decreases.

The SAXS-measured radius of gyration of primary particle (R_{g1}), radius of gyration of aggregate (R_{g2}), fractal dimension (d_f), and specific surface area (S) are plotted as a function of applied voltage in Figure 6. The aggregate sizes and specific surface areas are divided by 10 in Figure 6 in order to plot them on the same scale with primary particle size. As the applied voltage increases to 7 kV across the flame, the primary particle and aggregate size decrease sharply. Under an electric field, the particles are charged and repel each other. This repulsion of charged particles causes a reduction of coagulation rates, leading to smaller primary particles.[26,27] Furthermore, growth rates of mass fractal aggregates are retarded because the concentration of charged particles is decreased by electrostatic dispersion.[28]

The morphologies of all SiO_2 powders made under negative electric fields are nanoscale mass-fractals with fractal dimension between 1.7 and 1.9, which are composed of nanosized primary particles. All these nanoscale mass fractals seem to be grown by a diffusion-limited cluster−cluster aggregation process, as the fractal dimension of 1.8 is consistent with our measured fractal dimension. Smaller primary particles seem to form smaller mass-fractal aggregates with higher fractal dimension. The estimated specific surface area by SAXS increases with increasing applied voltage, consistent with the reduction of primary-particle size, and N_2 adsorption experiments.[17] The specific surface areas measured by SAXS were 291, 399, and 410 m^2/g; meanwhile, those by BET were 155, 225, and 275 m^2/g at 3, 7, and 9 kV, respectively.[17] Quantitative differences between BET and SAXS data can be explained by the fact that the specific surface area by X-ray scattering is based on the contrast difference between particles and background. Therefore, there is no limit to access area lost by interparticle bonding which N_2 in a gas adsorption measurement cannot access because of the finite size of N_2 molecules.

Similar scattering patterns are observed for SiO_2 powders produced under positive electric field using needle instead of plate electrodes. All of these SiO_2 powders are nanosize mass-fractals with d_f again between 1.5 and 1.9. The measured R_{g1}, R_{g2}, d_f, and S are plotted as a function of applied voltage in Figure 7. Similar to Figure 6, the electric field (Figure 7) also reduces aggregate and primary particle size. Since particles are charged, they repel each other, leading to reduction of the coagulation rate. Moreover, ionic winds[29] generated across the flame with needle electrodes reduce the particle residence time in the flame. As the field strength increases, the flame decreases in height and leans toward the cathode. Since the positive ions are larger than the electrons, the motion

(23) Witten, T. A.; Sander, L. M. *Phys. Rev. Lett.* **1981**, *47*, 1400.
(24) Brinker, C. J.; Scherer, G. W. *Sol−Gel Science; The Physics and Chemistry of Sol- Gel Processing*; Academic Press: New York, 1990; p 196.
(25) Vijayakumar, R.; Whitby, K. T. *Aerosol. Sci. Technol.* **1984**, *3*, 17.
(26) Zebel, V. G. *Kolloid-Z.* **1958**, *157*, 37.
(27) Fuchs, N. A. *The Mechanics of Aerosols*; Dover Publications: New York, 1964; p 288.
(28) Kasper, G. *J. Colloid Interface Sci.* **1981**, *81*, 32.
(29) Vemury, S.; Pratsinis S. E. *Appl. Phys. Lett.* **1995**, *66*, 3275.

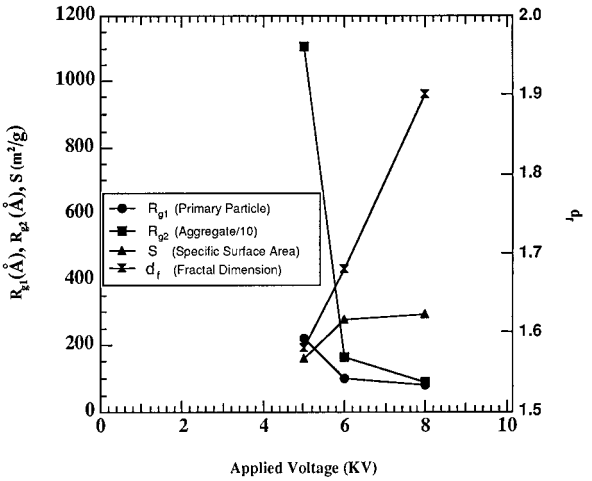

Figure 7. Radius of gyration of primary particle R_{g1}, radius of gyration of aggregates R_{g2}, specific surface area S, and fractal dimension d_f as a function of applied voltage across the flame for positive electric field with needles. The R_{g2} data have been divided by 10.

of positive ions "drags" neutral gas molecules, creating a net gas movement toward the cathode.[18,30] Reduced residence time and flame temperature[25] lead to smaller primary particles. Smaller primary particles again form smaller aggregates with higher fractal dimension as seen with plate electrodes. The measured fractal dimension falls between 1.6 and 1.8, and monotonically increases with the applied voltage between the electrodes, implying that the aggregates become denser. Particles with these mass-fractal dimensions seem to grow also by cluster−cluster aggregation processes. The measured specific surface areas by SAXS also increases with increasing applied voltage, consistent with N_2 adsorption again. The measured specific surface areas by SAXS were 158, 277, and 290 m^2/g; meanwhile, those by BET were 155, 175, and 190 m^2/g at 5, 6, and 8 kV, respectively.

Among unipolar electric fields, the negative electric field, Figure 6, is more effective in reducing particle sizes of both primary particles and aggregates. Particles are more efficiently charged under negative electric field because the velocity of negative ions are 20−50% faster than that of the positive ions.[31−33] As a result, particle growth by coagulation and coalescence seem to be retarded more effectively with negative than positive fields. This dramatically reduces particle sintering, resulting in smaller primary particle and higher specific surface area.

Conclusions

The morphology of flame-synthesized silica and titania aggregates were investigated with SAXS. Flame-generated titania aggregates are nanoscale mass fractals with fractal dimension near 1.7 in a laminar double diffusion flame reactors. Flame A generates the smallest primary particles and aggregates among four different kinds of flame reactors. In contrast, titania particles made in single diffusion flames are nonfractals and unaggregated. These results are consistent with TEM observations.

All flame-generated silica powders were mass-fractals regardless of the reactor type, oxidants, plate/needle configurations, and polarities of electric field. When oxygen was used as oxidant in a diffusion flame reactor, primary particles and aggregates are larger than those produced using air as oxidant. Moreover, the smaller the aggregates were, the higher the fractal dimensions obtained under the same flame configuration. The smaller primary particles were, the larger the measured surface area. When a unipolar electric field is applied across the flame in a laminar premixed flame reactor, silica powders show decreasing tendencies in primary particle and aggregate sizes as the applied voltage increases. Among unipolar electric fields, negative electric fields are more effective at reducing primary particle and aggregate size. The fractal dimension increases as applied voltage increases, with a range between 1.5 and 1.9 regardless of polarity.

Silica and titania aggregates synthesized in a diffusion flame reactor have a wide range of fractal dimensions from 2.5 to 1.6, implying that the main feature of particle growth follows a diffusion-limited monomer−cluster or a cluster−cluster mechanism. However, silica aggregates generated in the presence of electric fields in a laminar, premixed flame reactor have more narrowly confined fractal dimensions from 1.6 to 1.9, suggesting that all primary particles similarly grow by a diffusion-limited cluster−cluster aggregation mechanism.

Acknowledgment. This work was sponsored by the National Science Foundation, Grant CTS-9619392. SAXS was obtained at the UNM/Sandia scattering center with the assistance of Thomas Rieker. Grant CTS-9730535 also supported this work.

LA980308S

(30) Payne, K. G.; Weinberg, F. J. *Proc. R. Soc. London* **1959**, *A250*, 316.
(31) Adachi, M.; Kousaka, Y.; Okuyama, K. *J. Aerosol Sci.* **1985**, *16*, 109.
(32) Wiedensohler, A. *J. Aerosol Sci.* **1988**, *19*, 387.
(33) Bradley, D. In *Advanced Combustion Methods*; Weinberg, F. J., Ed.; Academic Press: Orlando, FL, 1986; p 331.